

# Static Solitary Waves in Axisymmetric Bose–Einstein Condensates

S. Komineas<sup>1</sup> and N. Papanicolaou<sup>2</sup>

<sup>1</sup> *Theory of Condensed Matter Group, Cavendish Laboratory, Madingley Road, Cambridge, CB3 0HE United Kingdom*  
 e-mail: sk407@cam.ac.uk

<sup>2</sup> *Department of Physics, University of Crete, and Research Center of Crete, Heraklion, Greece*

Received September 16, 2003

**Abstract**—Quasi-one-dimensional solitons that may occur in a confined axisymmetric Bose–Einstein condensate become unstable at high particle number. Here, we study two basic modes of instability and the corresponding bifurcations to axisymmetric vortex rings and nonaxisymmetric solitonic vortices, whose static profiles are calculated explicitly.

The possible occurrence of solitons in a Bose–Einstein condensate (BEC) was theoretically predicted some time ago within a one-dimensional (1D) Gross–Pitaevskii model [1, 2], while similar coherent structures were recently observed in BECs confined in traps of varying geometry [3, 4] by a method (phase imprinting) that was directly inspired by the analytical structure of 1D solitons. Yet it has become clear that quasi-1D solitons are susceptible to various instabilities within the three-dimensional (3D) environment of realistic traps.

A stability analysis based on the linear Bogoliubov–de Gennes (BdG) equations [5] revealed that an axisymmetric soliton is stable only at sufficiently low particle number or high aspect ratio in an elongated trap. The primary mode of instability was shown to result from nonaxisymmetric perturbations in the sense that a purely imaginary eigenvalue first appears in the spectrum of the BdG equations with azimuthal angular momentum  $m = 1$ . This “snake instability” was further analyzed in [6] and argued to be responsible for a possible decay of a soliton into vortex rings and/or vortices. Based on the above theoretical work, nonstationary vortex rings were experimentally detected in a spherical trap [7]. On the other hand, Brand and Reinhardt [8, 9] suggested that the primitive mode associated with the snake instability is a stable structure that may be called a solitonic vortex.

In recent works [10, 11], we carried out a detailed calculation of axisymmetric solitons in a cylindrical trap, which were shown to become unstable at high particle density even if we restrict ourselves to radial ( $m = 0$ ) perturbations. The soliton was then shown to bifurcate to an axisymmetric vortex ring with lower energy. The above work was completed in [12] by allowing azimuthal deformations of the soliton in order to eventually account for the primary ( $m = 1$ ) instability discussed in [5, 6]. We thus obtained a reasonably complete description of the two basic modes of instability and the corresponding bifurcations to axisymmetric

vortex rings and nonaxisymmetric solitonic vortices. The simplest theoretical picture was obtained [12] in the ideal limit of an infinitely elongated cylindrical trap, because static solitary waves may then be treated on equal footing with those propagating at nonzero velocity. Here, we focus on finite traps where the only true stationary states are the ground state and a variety of static solitary waves.

A finite axisymmetric harmonic trap is characterized by a transverse confinement frequency  $\omega_{\perp}$  and a longitudinal frequency  $\omega_{\parallel}$ . Rationalized physical units are introduced by measuring time in units of  $1/\omega_{\perp}$  and distance in units of the transverse oscillator length  $a_{\perp} = (\hbar/M\omega_{\perp})^{1/2}$ , where  $M$  is the mass of each atom. The wave function is rescaled according to  $\Psi \rightarrow \sqrt{N}\Psi/a_{\perp}^{3/2}$ , where  $N$  is the total number of atoms, and thus satisfies the constraint  $\int |\Psi|^2 dV = 1$ . The Gross–Pitaevskii equation then reads

$$i\frac{\partial\Psi}{\partial t} = -\frac{1}{2}\Delta\Psi + V_{\text{tr}}\Psi + g|\Psi|^2\Psi, \quad (1)$$

$$g = 4\pi\alpha, \quad V_{\text{tr}} = \frac{1}{2}(\rho^2 + \beta^2 z^2),$$

$$\rho^2 = x^2 + y^2$$

and is expressed entirely in terms of two independent dimensionless coupling constants, namely,  $\alpha = Na/a_{\perp}$ , where  $a$  is the scattering length, and  $\beta = \omega_{\parallel}/\omega_{\perp}$ . The conserved energy functional associated with Eq. (1) is then given by

$$W = \frac{1}{2}\int (|\nabla\Psi|^2 + 2V_{\text{tr}}|\Psi|^2 + g|\Psi|^4)dV \quad (2)$$

and yields energy in units of  $N(\hbar\omega_{\perp})$ .

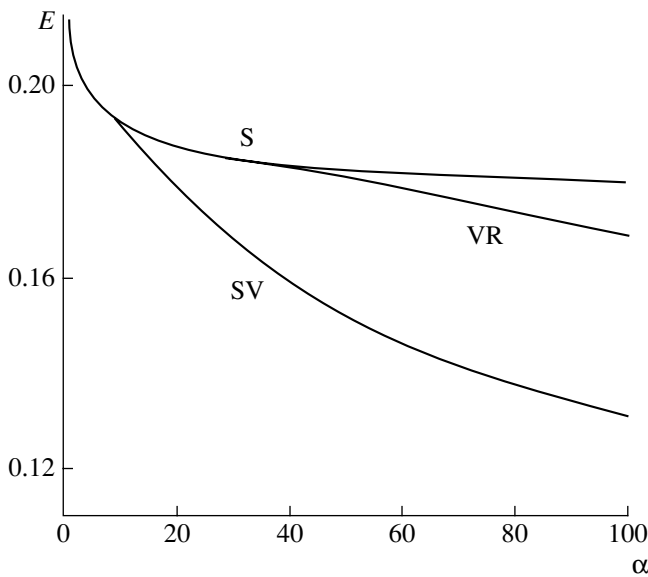


**Fig. 1.** Excitation energy  $E$  (in units of  $N\hbar\omega_{\perp}$ ) for a soliton (S), a solitonic vortex (SV), and a vortex ring (VR) as a function of the dimensionless coupling constant  $\alpha$  at fixed aspect ratio  $\beta = 1/4$ . Bifurcations occur at the two critical couplings  $\alpha_0 = 10$  and  $\alpha_1 = 39$ .

We now consider stationary states obtained by making the substitution  $\Psi(\mathbf{r}, t) \rightarrow e^{-i\mu t}\Psi(\mathbf{r})$  in Eq. (1) to derive the static equation

$$\mu\Psi = -\frac{1}{2}\Delta\Psi + V_r\Psi + g|\Psi|^2\Psi, \quad (3)$$

where  $\mu$  is the chemical potential (in units of  $\hbar\omega_{\perp}$ ) required to enforce a definite number of particles. Explicit solutions of Eq. (3) are calculated with a fully 3D iterative Newton–Raphson algorithm briefly described in our recent work [10–12].

The simplest and most important solution of Eq. (3) is the ground state  $\Psi = \Psi_0(\rho, z)$ , which is axially symmetric and even under the parity reflection  $z \rightarrow -z$ . The wave function  $\Psi_0$  provides the basis for all subsequent calculations but will not be illustrated explicitly in the present paper. Next, we consider an excited self-consistent state that is again axially symmetric,  $\Psi = \Psi_S(\rho, z)$ , but is now an odd function of  $z$ . Such a configuration is a 3D analog of the static (black) 1D soliton. It is interesting to consider the excitation energy  $E = W_S - W_0$ , where  $W_0$  and  $W_S$  are both calculated from Eq. (2) applied for the ground state  $\Psi_0$  and the soliton wave function  $\Psi_S$ , respectively. The excitation energy is depicted in Fig. 1 as a function of coupling strength  $\alpha$  at fixed aspect ratio  $\beta = 1/4$ .

For any given  $\beta$ , the soliton becomes unstable when  $\alpha$  exceeds a certain critical value. In fact, there exists a sequence of critical couplings  $\alpha_0 = \alpha_0(\beta)$ ,  $\alpha_1 = \alpha_1(\beta)$ , ... that correspond to bifurcations of the soliton to more complex states with lower energy. The critical coupling

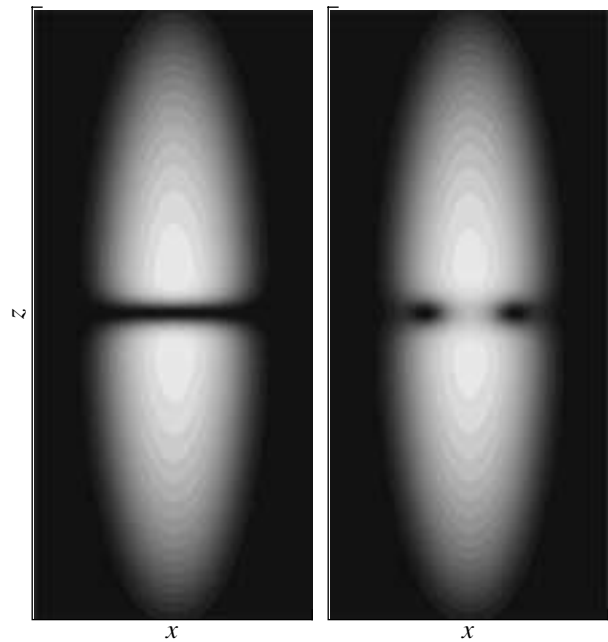


**Fig. 2.** Profiles of a static soliton (left panel) and a static vortex ring (right panel) on a finite trap with  $\alpha = 100$  and  $\beta = 1/4$  illustrated through density plots over a plane that contains the symmetry ( $z$ ) axis and cuts across the axisymmetric trap. The complete pictures can be obtained by simple revolution around the  $z$  axis because both the soliton and the vortex ring are axisymmetric.

$\alpha_0$  coincides with the coupling where a purely imaginary eigenvalue first appears in the  $m = 1$  sector of the linear BdG equations, and the corresponding bifurcation leads to the appearance of a nonaxisymmetric self-consistent state that may be called a solitonic vortex. Similarly, the critical coupling  $\alpha_1$  is related to an instability that occurs in the  $m = 0$  sector, but the picture is now significantly complicated by the appearance of complex modes [6]. Our numerical solution of the BdG equations shows that there exists an intermediate critical coupling  $\alpha'_1 < \alpha_1$  where two real eigenvalues with  $m = 0$  coalesce and eventually become complex for  $\alpha > \alpha'_1$ . The precise behavior of the complex eigenvalues with increasing  $\alpha$  depends on the specific value of  $\beta$ . A common feature is that complex eigenvalues as such again disappear before reaching the critical coupling  $\alpha_1$ . The latter is characterized by the fact that only one purely imaginary eigenvalue persists for  $\alpha > \alpha_1$  and signals a new bifurcation that leads to the appearance of axisymmetric vortex rings.

As an example, we consider the popular ratio  $\beta = 1/4$ , for which we find  $\alpha_0 = 10$ ,  $\alpha'_1 = 32$ , and  $\alpha_1 = 39$ . A static soliton exists for all  $\alpha$  but is stable only for  $\alpha < 10$ , while a static solitonic vortex appears for  $\alpha > 10$  with an energy that is lower than the soliton energy (see Fig. 1). A new threshold occurs at  $\alpha = 39$ , where a static

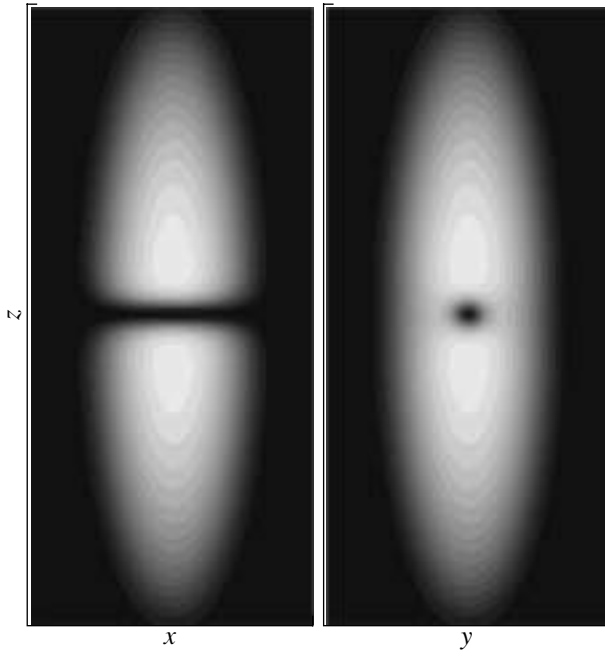


**Fig. 3.** Profile of a static solitonic vortex on a finite trap with  $\alpha = 100$  and  $\beta = 1/4$  illustrated through density plots over two planes that are perpendicular to each other and both contain the symmetry ( $z$ ) axis. Note that the solitonic vortex is not axisymmetric.

vortex ring emerges with energy intermediate between that of a soliton and a solitonic vortex. Explicit illustrations of the currently calculated profiles are given in Figs. 2 and 3 for  $\alpha = 100$  and  $\beta = 1/4$ , where all three types of static solitary waves are possible.

It is now interesting to discuss briefly how the preceding picture evolves with varying the aspect ratio  $\beta$ . We first consider the special limit of a spherical trap ( $\beta = 1$ ) in view of the experiment described in [7]. The critical coupling  $\alpha_0$  vanishes on a spherical trap, and thus the black soliton is not stable for any  $\alpha$ . On the other hand, the solitonic vortex now becomes degenerate with the ordinary vortex and is stable for all  $\alpha > 0$ . The vortex-ring threshold is here predicted to occur at  $\alpha_1 = 5$ . For the parameters of the actual experiment [7], we find  $\alpha = 430$ , which is substantially larger than  $\alpha_1$  and eventually explains the observation of multiple vortex rings. A single as well as a double vortex ring on a spherical trap are illustrated in Fig. 4. The double ring appears as two concentric rings in the reduced representation of the particle density plot. It is in fact a single self-consistent solution of the Gross–Pitaevskii equation.

In order to study the opposite limit of an infinitely elongated (cylindrical) trap ( $\beta \rightarrow 0$ ), it is useful to consider the average linear density  $v(z) =$

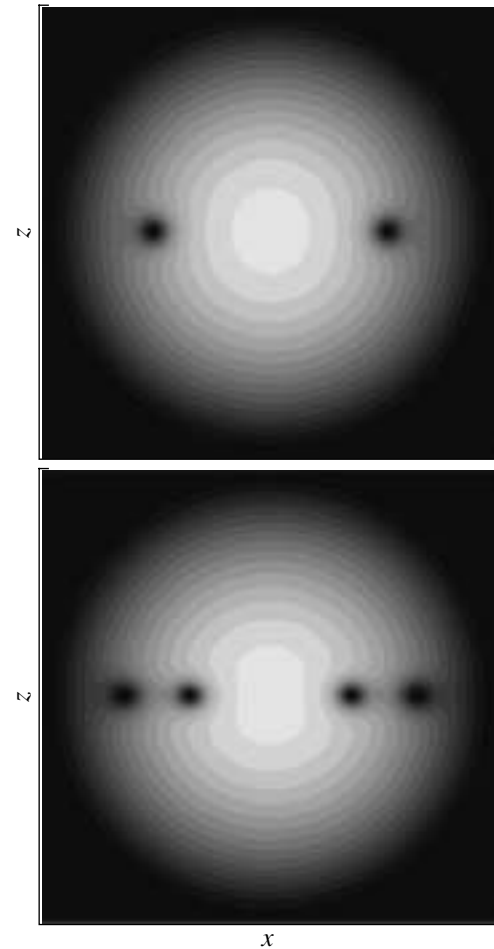


**Fig. 4.** Profiles of a single vortex ring (upper panel) and a double vortex ring (lower panel) in a spherical ( $\beta = 1$ ) trap with  $\alpha = 430$  illustrated through density plots over a plane that contains the symmetry ( $z$ ) axis and cuts across the spherical trap. The complete picture is obtained by simple revolution around the  $z$  axis because both the single and the double ring are axisymmetric.

$(N/\alpha_{\perp}) \int |\Psi|^2 dx dy$  and then define the dimensionless quantity  $\gamma(z) = av(z)$  or

$$\gamma(z) = \alpha \int |\Psi|^2 dx dy. \quad (4)$$

The function  $\gamma(z)$  becomes increasingly uniform in the limit  $\alpha \rightarrow \infty$ ,  $\beta \rightarrow 0$ , holding  $\gamma(0) \equiv \gamma$  fixed, which is the ideal limit of the infinite cylindrical trap primarily studied in [10–12]. Both critical couplings  $\alpha_0(\beta)$  and  $\alpha_1(\beta)$  increase indefinitely in the above limit, but the corresponding critical couplings calculated from  $\gamma(0)$  reach the finite values  $\gamma_0 \approx 1.5$  and  $\gamma_1 \approx 4$ .

As a simple illustration, we consider the Thomas–Fermi (TF) approximation of the ground state [13] to find that

$$\gamma(z) = \frac{1}{16} (2\mu - \beta^2 z^2)^2, \quad (5)$$

where the chemical potential is given by  $2\mu = (15\alpha\beta)^{2/5}$ . Therefore, the estimated maximum value of  $\gamma$  is given by  $\gamma_{\max} = \gamma(0) = \mu^2/4$ . A more conservative estimate is the average value defined from  $\gamma_{\text{av}} = \alpha/L$ , where  $L = 2\sqrt{2\mu}/\beta$  is the TF length of the trap and thus  $\gamma_{\text{av}} = (8/15)\gamma_{\max}$ . The TF radius of the trap is given accordingly by  $R = \sqrt{2\mu}$ . For the parameters of the experiment described in [3], we find  $R = 2 \mu\text{m}$  and  $L = 115 \mu\text{m}$ , while  $\gamma_{\max} = 13$  and  $\gamma_{\text{av}} = 7$ . By both estimates, the value of  $\gamma$  exceeds the critical coupling  $\gamma_1 = 4$ . Therefore, all three types of solitary waves (solitons, solitonic vortices, and vortex rings) should have been produced in the experiment described in [3].

#### REFERENCES

1. T. Tsuzuki, *J. Low Temp. Phys.* **4**, 441 (1971).
2. V. E. Zakharov and A. B. Shabat, *Sov. Phys. JETP* **37**, 823 (1973).
3. S. Burger, K. Bongs, S. Dettmer, *et al.*, *Phys. Rev. Lett.* **83**, 5198 (1999).
4. J. Denschlag, J. E. Simsarian, D. L. Feder, *et al.*, *Science* **287**, 97 (2000).
5. A. E. Muryshev, H. B. van Linden van den Heuvell, and G. V. Shlyapnikov, *Phys. Rev. A* **60**, R2665 (1999).
6. D. L. Feder, M. S. Pindzola, L. A. Collins, *et al.*, *Phys. Rev. A* **62**, 053 606 (2000).
7. B. P. Anderson, P. C. Haljan, C. A. Regal, *et al.*, *Phys. Rev. Lett.* **86**, 2926 (2001).
8. J. Brand and W. P. Reinhardt, *J. Phys. B* **34**, L113 (2001).
9. J. Brand and W. P. Reinhardt, *Phys. Rev. A* **65**, 043 612 (2002).
10. S. Komineas and N. Papanicolaou, *Phys. Rev. Lett.* **89**, 070402 (2002).
11. S. Komineas and N. Papanicolaou, *Phys. Rev. A* **67**, 023 615 (2003).
12. S. Komineas and N. Papanicolaou, cond-mat/0304123, *Phys. Rev. A* (in press).
13. G. Baym and C. J. Pethick, *Phys. Rev. Lett.* **76**, 6 (1996).